Published in final edited form as:
J Am Chem Soc. 2007 May 9; 129(18): 5910–5918.

Turn-On and Ratiometric Mercury Sensing in Water with a Red-Emitting Probe

Elizabeth M. Nolan and **Stephen J. Lippard***
Department of Chemistry, Massachusetts Institute of Technology, Cambridge, MA 02139

Abstract

The synthesis, photophysical properties, and Hg(II)-binding of a red-emitting sensor for mercuric ion are presented. MS5, 2-{11-[(2-{[bis-(2-ethylsulfanylethyl)-amino]methyl}phenylamino) methyl]-3-hydroxy-10-oxo-10H-benzo[c]xanthen-7-yl}-benzoic acid, is based on the seminaphthofluorescein chromophore and employs a thioether-rich metal-binding unit. This sensor affords both turn-on and single-excitation dual-emission ratiometric Hg(II) detection in aqueous solution. The fluorescence response of MS5 is Hg(II)-specific and the probe is selective for Hg(II) over alkali and alkaline earth metals, most divalent first-row transition metal ions, and the Group 12 congeners Zn(II) and Cd(II). MS5 binds Hg(II) reversibly and can be recycled. The EC_{50} for 1 μM MS5 is 910 nM and a lower detection limit of 50 nM is obtained when employing 500 nM probe. X-ray crystallographic studies using a salicylaldehyde-based model of MS5 are also presented. 2-[2-{[Bis-(2-ethylsulfanylethyl)amine]methyl}phenylamine)methyl]phenol coordinates Hg(II) with two thioether sulfur atoms, two amino nitrogen atoms, and a phenol oxygen atom arranged in a distorted trigonal bipyramidal geometry. Studies of natural water samples spiked with mercuric salts indicate that MS5 can rapidly detect Hg(II) in such complex solutions and demonstrate its potential utility in the field.

Introduction

A variety of natural and anthropogenic environmental contaminants pose serious problems for human health and ecology. Mercury pollution is a topic of recent concern[1–6] and has sparked interest in the design of new chemical tools and tactics for its detection. Small molecule sensors that provide selective and immediate response to Hg(II), observable visually or with simple spectroscopic instrumentation, are particularly valuable. Such probes can ultimately be employed in basic laboratory assays, adapted for measurements in the field through their incorporation into portable fiber optic devices and, as is the case for Pb(II) detection, fabricated into commercial indictors for household use.

Fluorescence is a powerful optical technique for detecting low concentrations of analytes. A number of fluorescence-based Hg(II) probes have been reported and include polymers,[7,8] foldamers,[9] biomolecules,[10–12] and small molecules.[13–32] Many fluorescent small-molecule Hg(II) sensors presented to date are quenched upon Hg(II) coordination, rely on an irreversible Hg(II)-dependent chemical reaction to give fluorescence turn-on, and/or require organic solvent systems, features that may be problematic depending on a given application. Achieving water compatibility is important[33] and often a challenge in Hg(II) sensor design. Recently, significant efforts have been made to prepare Hg(II)-sensitive molecules that operate in purely aqueous solution and afford fluorescence enhancement and/or a ratiometric response.[34–44] Many of these detectors utilize fluorescein,[35,43] rhodamine,[37,40,44] BODIPY,[42] or

*To whom the correspondence should be addressed: lippard@mit.edu.

naphthalmide[38] reporting groups and exhibit emission in the visible region of the spectrum with $\lambda_{max} \leq 560$ nm. Examples of Hg(II) sensors with lower energy emission are limited. A phenoxazinone appended with a thioether-rich macrocycle affords maximum emission at ca. 600 nm in aqueous solution, but Hg(II) coordination results in fluorescence quenching.[45] MS4 (Figure 1) exhibits emission enhancement centered at 624 nm following Hg(II) binding, but the change is small (~2-fold) at neutral pH.[35]. Two probes that respond to Hg(II) and give near infrared emission in organic solvents have been reported, but their applicability to aqueous milieu was not documented.[46,47] Designing improved Hg(II) sensors that emit at relatively long wavelengths, exhibit Hg(II) sensitivity and selectivity, and have a robust and immediate response to Hg(II) in water is an important goal. Such probes will be useful in a number of applications, including multi-color analyses requiring sensors that emit at different wavelengths.

In the present article, we address this need and present the synthesis and characterization of Mercury Sensor 5 (MS5, Scheme 1). This sensor is based on a seminaphthofluorescein chromophore, which is water-compatible and affords red-shifted emission relative to fluorescein, rhodamine, and other commonly used reporters. Given the high affinity of Hg(II) for soft sulfur donors, we chose to incorporate the thioether-rich metal-binding unit previously designed for fluorescein-based MS1 (Figure 1). Because of these design features, MS5 has a number of advantageous features that include (i) turn-on and ratiometric Hg(II) detection, (ii) rapid and Hg(II)-specific fluorescence response, (iii) reversibility, and (iv) a detection limit for Hg(II) in the nM range. In addition, MS5 exhibits selectivity for Hg(II) over many competing species, including those found in natural water samples.

Experimental Section

Reagents

Anhydrous methanol, chloroform, and 1,2-dichloroethane (DCE) were purchased from Aldrich and used as received. Sodium triacetoxyborohydride and mercury(II) perchlorate hydrate were also obtained from Aldrich. *N′*,*N′*,*N″*,*N″*-tetrakis(2-picolyl)ethylenediamine (TPEN) was purchased from Invitrogen. The aniline derivatized ligand **1**[34] and seminaphthofluorescein aldehyde **2**[48] were synthesized according to previously published procedures. A portion of 2-(10-hydroxy-3-phenylaminomethyl-3H-benzo[c]xanthen-7-yl)benzoic acid, **3**, a synthetic precursor to **2**, was prepared as described in the literature[48] and further purified by preparative TLC on silica gel (20:1 $CHCl_3$/MeOH) for use in spectroscopic studies.

CAUTION—The isolated Hg(II) complexes described below contain perchlorate ion, which can detonate explosively and without warning. Although we encountered no problems with the isolated compounds, all due precautions should be taken.

Materials and Methods

Merck 254 silica gel 60 plates (0.25 mm thickness) were used for analytical thin-layer chromatography (TLC) and were viewed with UV light. Whatman silica gel 60 plates (1 mm thickness) were used as the solid phase for preparative TLC. NMR spectra were collected on a Varian 300 or 500 MHz spectrophotometer and the spectra were referenced to internal standards. An Avatar FTIR instrument was used to obtain IR spectra. High-resolution mass spectra were collected by staff at the MIT Department of Chemistry Instrumentation Facility.

2-{11-[(2-{[Bis-(2-ethylsulfanylethyl)amino]methyl}phenylamino)methyl]-3-hydroxy-10-oxo-10H-benzo[c]xanthen-7-yl}benzoic acid (4, MS5)

To 9 mL of a 7:2 $CHCl_3$/MeOH mixture were added **1** (71 mg, 0.17 mmol) and **2** (52 mg, 0.17 mmol), which gave a red-brown solution that was stirred at room temperature. After 24 h, 3

mL of DCE and $NaB(OAc)_3H$ (40 mg, 0.19 mmol) were added and the reaction was stirred for an additional 24 h, during which time it became wine-colored. The solvents were removed under reduced pressure and preparative TLC on silica gel (20:1 $CHCl_3$/MeOH) yielded pure MS5 as a purple solid (38 mg, 32%). TLC R_f = 0.64 (9:1 $CHCl_3$/MeOH); mp > 300 °C, dec. ^1H NMR (CD_3OD, 500 MHz) δ0.94 (6H, t), 2.08 (4H, m), 2.24 (4H, m), 2.39 (2H, m), 2.47 (2H, m), 3.55 (2H, s), 4.70 (2H, q), 6.64 (1H, t), 6.71 (1H, d), 6.92 (1H, d), 6.98 (3H, m), 7.13 (1H, d), 7.20 (1H, d), 7.28 (2H, m), 7.34 (1H, m), 7.61 (2H, m), 8.10 (1H, d), 8.27 (1H, m). FTIR (KBr, cm^{-1}) 3428 (w, br), 3052 (w), 2957 (w), 2921 (w), 2857 (w), 2800 (w), 1752 (w), 1641 (m), 1600 (s), 1585 (s), 1563 (m), 1504 (m), 1470 (s), 1443 (s), 1377 (m), 1339 (m), 1309 (m), 1251 (m), 1143 (m), 1091 (m), 1070 (w), 1046 (w), 1004 (w), 961 (w), 931 (w), 877 (w), 862 (w), 827 (w), 789 (w), 748 (w), 726 (w), 704 (w), 678 (w), 643 (w), 613 (w), 596 (w), 526 (w), 448 (w). HRMS (ESI) Calcd $[M - H]^-$, 691.2306; Found, 691.2325.

2-[2-{[Bis-(2-ethylsulfanylethyl)amine]inethyl}phenylamine)inethyl]phenol (5,L)

Salicylaldehyde (376 mg, 3.08 mmol) and *N*-(2-aminobenzyl)-3,9-dithia-6-azaundecane (**1**, 914 mg, 3.07 mmol) were combined in 40 mL of EtOAc and stirred for 10 h at room temperature. The solvent was removed in vacuo to yield an orange-yellow oil. The oil was dissolved in 30 mL of DCE and $NaB(OAc)_3H$ (700 mg, 3.33 mmol) was added. The reaction was stirred overnight at room temperature, diluted with 40 mL of dichloromethane, and washed with saturated brine (3 × 80 mL) and then water (1 × 80 mL). The organic portion was dried over $MgSO_4$ and the solvent was removed to yield an orange oil. Chromatography on $A1_2O_3$ with a solvent gradient (2:1 hexanes/EtOAc to 100% EtOAc) afforded the product as an orange oil that solidified upon cooling at 4 °C (812 mg, 65%). TLC R_f = 0.60 ($A1_2O_3$, 2:1 hexanes/EtOAc). ^1H NMR ($CDCl_3$, 300 MHz) δ 1.17 (6H, t), 2.37 (4H, q), 2.58 (4H, m), 2.65 (4H, m), 3.70 (2H, s), 4.48 (2H, s), 6.78–6.91 (4H, m), 7.05 (1H, dd), 7.16–7.23 (3H, m). ^{13}C NMR ($CDCl_3$,125 MHz) δ 14.79, 25.88, 29.34, 47.65, 53.02, 58.35, 113.18, 116.33, 119.25, 119.75, 123.64, 124.72, 128.57, 128.90, 130.29, 147.42, 157.16. FTIR (NaCl disk, cm^{-1}) 3217 (s, br), 3043 (s), 2963 (s), 2924 (s), 2869 (s), 2845 (s), 2817 (s), 2717 (w), 1606 (s), 1588 (s), 1508 (s), 1490 (s), 1455 (s), 1375 (m), 1314 (m), 1294 (m), 1250 (m), 1149 (w), 1119 (m), 1102 (m), 1050 (m), 1036 (m), 983 (m), 932 (m), 855 (m), 839 (m), 753 (s), 723 (m), 658 (w), 629 (w), 565 (w), 531 (w). HRMS (ESI) Calcd $[M + H]^+$, 405.2029; Found, 405.2019.

[Hg(L)]$(ClO_4)_2$·CH_3OH (6)

A portion (9.7 mg, 0.024 mmol) of $Hg(ClO_4)_2·H_2O$ was suspended in 0.5 mL of MeOH to which a solution of **5** (10 mg, 0.025 mmol) in 0.5 mL of MeOH was added dropwise as the solution turned yellow. The solution was sonicated for 5 min and filtered. Colorless thin needle crystals suitable for X-ray crystallographic analysis formed over the course of 48 h by vapor diffusion of Et_2O into the reaction at room temperature. The solvents were decanted and the crystals washed with Et_2O (4×3 mL) and dried in vaco (11.5 mg, 48%). FTIR (KBr, cm^{-1}) 3546 (m, br), 3192 (m, br), 3069 (w), 2969 (w), 2932 (w), 2865 (w), 2835 (w), 2700 (w), 2605 (w), 2552 (w), 1609 (m), 1594 (m), 1496 (m), 1460 (s), 1421 (m), 1384 (120m), 1368 (m), 1300 (w), 1258 (m), 1218 (w), 1188 (w), 1102 (s, br), 1084 (s), 1055 (s), 1047 (s), 1004 (m), 932 (m), 922 (m), 910 (m), 884 (m), 870 (m), 853 (m), 832 (w), 801 (w), 770 (s), 729 (w), 717 (m), 672 (w), 622 (s), 575 (w), 543 (w), 521 (w), 494 (w), 484 (w), 468 (w). HRMS (ESI) Calcd $[M–2(ClO_4)–H]^+$, 605.1584; Found, 605.1578. Anal: Calcd for $C_{23}H_{36}Cl_2N_2O_{10}S_2Hg$: C, 33.04; H, 4.34; N, 3.35. Found: C, 33.01; H, 4.44; N, 3.30.

[Hg(TPEN)]$(ClO_4)_2$ (7)

A portion (7.8 mg, 0.195 mmol) of $Hg(ClO_4)_2·H_2O$ in 1 mL of MeOH was added dropwise to a solution of TPEN (7.9 mg, 0.184 mmol) in 1 mL of MeOH. The solution was mixed with a pipette and filtered. Colorless rod-like crystals suitable for X-ray crystallography formed over

the course of 48 h from vapor diffusion of Et_2O into the reaction mixture at room temperature. The solvents were decanted and the crystals were washed with Et_2O (4×3 mL) and dried in vacuo (8.6 mg, 57%). FTIR (KBr, cm^{-1}) 3107 (w), 3078 (w), 3033 (w), 2963 (w), 2936 (w), 2911 (w), 2895 (w), 2859 (w), 1600 (m), 1572 (w), 1486 (m), 1467 (m), 1455 (m), 1441 (m), 1386 (w), 1374 (w), 1335 (w), 1318 (w), 1300 (w), 1294 (w), 1263 (m), 1221 (w), 1159 (w), 1130 (m), 1095 (vs), 1067 (s), 1051 (s), 1015 (m), 991 (m), 974 (w), 939 (w), 930 (w), 897 (w), 866 (w), 841 (w), 802 (m, br), 764 (m), 734 (w), 723 (w), 646 (w), 621 (m), 584 (w). HRMS (ESI) Calcd M^{2+}, 313.1040; Found, 313.1054. Anal: Calcd for $C_{26}H_{28}Cl_2HgN_2O_8$: C, 37.90; H, 3.42; N, 10.20. Found: C, 37.96; H, 3.23; N, 10.25.

X-ray Crystallographic Studies

Single crystals were mounted on the tips of glass fibers coated with Paratone-N oil and cooled to −100 °C under a stream of N_2 maintained by a KRYO-FLEX low-temperature apparatus. Intensity data were collected on a Bruker APEX CCD diffractometer with graphite-monochromated Mo Kα radiation (λ, = 0.71073 Å), controlled by a Pentium-based PC running the SMART software package.[49] Data collection and reduction protocols are described elsewhere.[50] Empirical absorption corrections were applied by using the SADABS[51] program and the structures were solved by direct methods using the SAINTPLUS[52] and SHELXTL[53] software packages. The structures were checked for higher symmetry by using the PLATON software package.[54] All non-hydrogen atoms were located and their positions refined with anisotropic thermal parameters by least-squares cycles and Fourier syntheses. Unless otherwise noted, hydrogen atoms were assigned to idealized positions and given thermal parameters equivalent to either 1.5 (methyl hydrogen atoms) or 1.2 (all other hydrogen atoms) times the thermal parameter of the carbon atom to which they were attached. The structure of 6 includes one ordered methanol and two ordered perchlorate anions. The O1 and N1 hydrogen atoms of **6** were located from an electron density map. The structure of **7** includes two ordered perchlorate groups.

Spectroscopic Materials and Methods

Millipore water (18.2 Mω·cm at 25 °C) obtained from a Milli-Q Biocel purifier outfitted with a Quantum VX cartridge was used to prepare all aqueous solutions. PIPES, piperazine-*N*,*N*′-bis(2-ethanesulfonic acid), CHES, 2-(*N*-cyclohexylamino)ethanesulfonic acid, and CABS, 4-cyclohexylamino-1-butanesulfonic acid, buffers were purchased from Sigma and used as received. Puratonic grade KCl was purchased from Calbiochem. Mercury stock solutions (10 mM) were prepared from 99.998% anhydrous $HgCl_2$ (Aldrich) and water. DMSO stock solutions of **3** (2 mM, deep red-purple) and MS5 (1 mM, deep purple) were prepared, partitioned into ~40 μL aliquots, stored at −25 °C, and thawed in the dark immediately before use. For measurements conducted in buffered solutions the buffer concentration was 50 mM and, with the exception of the anion variation experiments, 100 mM KCl. The pH titrations were conducted in the presence of 100 mM KCl. Quantum yields were measured relative to fluorescein in 0.1 N NaOH (Φ = 0.95),[55] Experimental details for all spectroscopic measurements are available elsewhere.[34,43] All measurements were repeated a minimum of three times and the resulting averages are reported.

Fluorescence spectra were collected by using a Photon Technology International (Lawrenceville, NJ) Quanta Master 4L-format scanning spectrofluorimeter equipped with an LPS-220B 75-W xenon lamp and power supply, A-1010B lamp housing with integrated igniter, switchable 814 photon-counting/analog PMT detector, and a MD-5020 motor driver. Optical absorption spectra were collected on a Gary IE double-beam scanning spectrophotometer. All samples were contained in 3 mL quartz cuvettes with 1-cm path lengths (Starna) and maintained at 25 °C by means of a circulating water bath.

Water Collection

Natural water samples from the Charles River (Cambridge, MA), Onondaga Lake (New York state), and the harbor in Newburyport, MA were collected in August 2005 and stored in polypropylene bottles. The water samples were passed through 0.2 μm filters to remove particulate and insoluble organic matter prior to use.

Results and Discussion

Design and Synthesis of MS5

Several considerations influenced the design of sensor MS5. Our first objective was to employ a fluorophore with relatively low-energy emission relative to fluorescein and other commonly employed chromophores. Metal ion sensors based on seminaphthofluorescein **3** (Figure 1) offer maximum emission at >600 nm in aqueous solution, a feature beneficial for applications requiring multicolor detection and for biological use where lower energy excitation is preferred. A second objective was to obtain a sensor with high selectivity for Hg(II) compared to other metal ions. Ligand **1** was previously employed in the synthesis of MS1 (Figure 1) and confers better selectivity for Hg(II) than metal-coordinating groups with fewer sulfur donor atoms. Scheme 1 shows the final transformation in the nine-step assembly of MS5. Combination of aniline **1** and aldehyde **2** in a mixed $CHCl_3$/MeOH solvent followed by imine reduction using $NaB(OAc)_3H$ afforded sensor MS5 in 32% yield as a dark purple powder following purification by preparative TLC on silica gel (20:1 $CHCl_3$/MeOH).

We also prepared a salicylaldehyde-based analogue of MS5, **L**, shown in Scheme 1, for use in X-ray crystallographic modeling studies. Ligand **L** was obtained in 65% yield as an off-white solid following Schiff base condensation of salicylaldehyde with aniline **1** and reduction with $NaB(OAc)_3H$ in DCE.

Spectroscopic Properties and Hg(II) Response of MS5

Like fluorescein, seminaphthofluorescein (SNAFL)[56] chromophores exhibit pH-sensitive absorption and emission spectra. The pH 7 to 9 range is particularly important because seminaphthofluorescein platform **3** (Figure 1) undergoes a fluorescence change corresponding to a pK_a of ~ 8 in aqueous solution containing 100 mM KCl (Figure S1, Supporting Information). Decreasing the pH in this range results in fluorescence quenching (Figure S1). This behavior is similar to the fluorescence quenching observed upon protonation of fluorescein, namely, fluorescence quenching (pK_a ~ 6.4). The corresponding changes in the optical absorption spectra, depicted in Figure S2, are also analogous to those observed upon fluorescein protonation to form the fluorescein monoanion.[57] From these comparisons, we conclude that the seminaphthofluorescein monoanion is the predominant species at pH 7 whereas the more emissive dianion is present at higher pH.

We next describe the spectroscopic characteristics and Hg(II) response of MS5 at pH ≥: 7. Table 1 lists the absorption and emission properties of MS5 in the absence and presence of excess Hg(II). The changes in optical absorption of free MS5 as a function of pH are comparable to those of **3**. There are two local maxima (500, 528 nm) of similar intensity at pH 7 and one red-shifted local maximum (552 nm) of much greater intensity at pH 9 (Figure S3). Similar pH-dependent trends are observed for the MS5:Hg(II) complex (Table 1, Figure S3).

The emission spectrum of free MS5 shows some variations with pH that differ from those of **3**. At pH ≥ 9, MS5 exhibits two emission bands centered at ca. 524 and 624 nm of similar intensity (Figure 2). Decreasing the pH to ~6 enhances the 524 nm band and reduces the 624 nm band with an isoemissive point at 600 nm. Further acidification results in fluorescence quenching. A ~50% increase in integrated emission occurs as the pH is lowered from ~9 to ~6,

which contrasts with the fluorescence decrease observed for **3** with increasing acidity. This behavior is similar to that observed for other metal-ion sensors containing aniline-derivatized ligands, including fluorescein-based MS1[34] and seminaphthofluorescein-based ZNP1 (Figure 1).[48,58] We attribute the effect to protonation of the aniline unit, which disrupts photoinduced electron transfer quenching. The quantum yields for apo MS5 were determined in the pH 7 to 9 range and are sensitive to pH changes in this interval. At pH 7, Φ_{free} is 0.018 and its magnitude decreases to ca. 0.01 at pH ≥ 8.

The fluorescence of MS5 is enhanced upon Hg(II) coordination at pH ≥ 7. Values for Φ_{Hg} are listed in Table 1 and representative emission spectra obtained for MS5 before and after Hg(II) addition at pH 7, 8, and 9 are given in Figure 3. At pH 7, an ~4-fold fluorescence enhancement occurs following Hg(II) coordination (Φ_{Hg} = 0.032). At pH 8 (Φ_{Hg} = 0.064) and 9 (Φ_{Hg} = 0.086) the increase in integrated emission is more dramatic, with a ~9- and ~11-fold turn-on, respectively. Interestingly, the nature of the fluorescence enhancement depends on pH. Significant increases in both the 524 and 624 nm emission bands contribute to the fluorescence turn-on at pH ≤ 8. At higher pH, Hg(II) coordination gives rise to only negligible changes in the 524 nm band, with dramatic increases at 624 nm. This property affords single-excitation dual-emission ratiometric detection of Hg(II) at pH > 8 through comparison of the ratio of the 524 and 624 nm ($\lambda_{,624}/\lambda_{,524}$) bands before and after Hg(II) addition ($\lambda_{,ex}$ = 499 nm). For instance, an ~13-fold ratio change occurs at pH 9. This feature may facilitate quantification in applied work.

The data included in Table 1 indicate that the greater dynamic range in the fluorescence response resulting from Hg(II) coordination at higher pH primarily stems from brighter Hg(II) complexes rather than reduced background emission. This observation contrasts the well-documented behavior of many proton-sensitive PET-based sensors, which display significantly reduced emission in alkaline solution.[59,60] Although the photophysical details of this phenomenon warrant further investigation, we propose that the underlying cause of the behavior stems from the protonation state of the seminaphthofluorescein platform and that the seminaphthofluoresein dianion is required for brighter emission from the MS5:Hg(II) complex. At pH 7, the seminaphthofluorescein is protonated and monoanionic, hence less emissive. Coordination of MS5 to Hg(II) does not promote deprotonation of this moiety (vide infra) and, although fluorescence turn-on occurs, emission from the weakly fluorescent monoanonic form of the seminaphthofluorescein results. At pH > 8, the seminaphthofluorescein is predominantly in its dianionic and most emissive form. The aniline unit effectively quenches its emission, as evidenced by the Φ_{free} values in Table 1, and Hg(II) coordination restores emission from the dianion.

As observed for MS1–4, the fluorescence response of MS5 to Hg(II) is sensitive to the presence of chloride ion. Figure 4 shows the fluorescence response of MS5 to Hg(II) in the presence and absence of chloride ion at pH 8. In 50 mM HEPES, an ~3-fold fluorescence enhancement occurs upon Hg(II) coordination, and subsequent introduction of 50 mM chloride ion immediately evokes full turn-on. Substitution of KCl with KX (X = NO_3^-, OAc^-, F^-) reveals that this effect is chloride-ion specific, although acetate also gives some emission enhancement. The presence of chloride ion has no effect on the emission of the free sensor. We have encountered such chloride ion dependence for Hg(II) sensors with a variety of ligand frameworks and have proposed that formation of a Hg–Cl bond or strong ion pairing influences the degree of turn-on in these systems.[34,35,43] Nevertheless, such chloride ion dependence is not completely general. For instance, some xanthenone-substituted Zinpyr sensors that contain di-(2-picolyl)amine ligands, such as ZP3 (Figure 1), give fluorescence enhancement following Hg(II) coordination and the degree of turn-on is independent of chloride ion in the buffer.[58] Fluo-5N, a sensor sold by Invitrogen, gives fluorescence turn-on for Hg(II) and the response is enhanced ~2.5-fold by substituting chloride with nitrate ion (50 mM PIPES, 100 mM KX,

pH 7).[58] These observations indicate that buffer composition must be considered when evaluating the response of fluorescent metal ion sensor.

Hg(II) Binding and Selectivity Studies

MS5 and MS1 share the same N_2S_2O set of chelating donor atoms. A 1:1 binding stoichiometry was previously observed in solution for Hg(II) complexation to MS1. In this work, we prepared a salicylaldehydebased model complex, **L** (Scheme 1), with the aim of elucidating further details about the likely mode of Hg(II) coordination to these sensors. X-ray quality crystals were obtained by vapor diffusion of Et_2O into a methanolic solution containing a 1:1 **L**/Hg$(ClO_4)_2$ mixture at room temperature. Tables S1 and S2 contain crystallographic data from the refinement as well as selected bond lengths and angles, respectively, for the **L**:Hg(II) complex **6**. The unit cell contains the mercury complex, two perchlorate anions, and one molecule of methanol. The N(1) and O(1) hydrogen atoms were located from an electron density map. An ORTEP diagram of **6** (Figures 5 & S5) reveals the Hg(II) center to be five-coordinate with a distorted trigonal bipyramidal geometry. The protonated phenol oxygen and tertiary amine nitrogen atoms are in the axial positions and the two thioether donors and the protonated aniline nitrogen atom form the equatorial plane. The Hg–S(1) and Hg–S(2) bond lengths are 2.5076 (8) and 2.4854(8) Å, respectively. These values are within the general 2.47 – 2.73 A range for Hg(II)-S(thioether) bonds and indicate strong Hg-S interactions.[61] The Hg–O(1) bond length of 2.572(3) Å suggests a relatively weak interaction. The Hg–N(2) distance, 2.436(3) Å, is slightly longer than that of the analogous Hg-N bond in [Hg(beppa)(ClO_4)]ClO_4, where beppa = {*N*,*N*-bis(2-ethylthio)ethyl-*N*-[(6-pivaloylamido-2-pyridyl)methyl]amine, and the bond length of relevance is 2.412(6) Å.[66] Overall, the structure of **6** is similar to that of [(beppa)Hg(ClO_4)]ClO_4, although mercury in the latter is described as six-coordinate because of a weak interaction with a perchlorate ion (3.01 Å). The beppa ligand itself provides a distorted trigonal bipyramidal geometry, where the tertiary amine and amide oxygen atoms are in the axial positions and two thioether donors and a pyridyl nitrogen atom lie in the equatorial plane. The perchlorate groups of 6 are non-interacting, the closest Hg–$OClO_3$ interaction being 3.87 Å. Although the model compound **6** suggests a five-coordinate geometry for the Hg(II) complex of MS5, in aqueous solution a water molecule (neutral pH) or hydroxide ion (basic pH) might be weakly associated with, if not bound to, the Hg(II) center.

The EC_{50}, or concentration of Hg(II) required to bring about 50% of the maximum fluorescence enhancement for a 1 μM solution of the probe, was determined for MS5 at pH 7 (50 mM PIPES, 100 mM KCl). The maximum fluorescence enhancement occurs in the presence of ~10 equiv of Hg(II) and the EC_{50} value is 910 nM (Figure S6). Despite the conserved metal binding unit, this value is higher than that of MS1 (EC_{50}= 410 nM, pH 7). The difference may reflect different protonation states of the fluorescein (MS1) and seminaphthofluorescein (MS5) platforms at pH 7, with phenolate coordination to Hg(II) for MS1 and phenol coordination to MS5. When a 0.5 μM solution of MS5 and 4 nm slit widths were employed, a lower detection limit of 50 nM Hg(II) was obtained at pH 7 (21% ± 4.5% fluorescence enhancement, mean ± SD for 16 trials).[62]

Binding of MS5 to Hg(II) is readily reversible. Addition of TPEN to solutions of MS5 and Hg (II) caused an immediate fluorescence decrease to within ~20% of the baseline value (Figure 6). This behavior is expected because TPEN has a reported K_d value of ~10^{-25} M for Hg(II) at 100 mM ionic strength.[63] Consecutive additions of Hg(II) and TPEN revealed that this on/off behavior could be cycled a number of times (Figure 6). Addition of excess KI(aq) also reverses the Hg(II) binding (data not shown).[43,64] Such reversibility and regeneration are important for the fabrication of devices to sense mercuric ion.

No crystal structure determination of a TPEN:Hg(II) complex has been published to date and structures of TPEN:Zn(II) complexes have only recently been reported.[65] Colorless X-ray

quality block crystals were grown from vapor diffusion of Et_2O into a methanolic solution of 1:1 TPEN/$Hg(ClO_4)_2$. ORTEP diagrams of **7** are given in Figures 5 and S7; Tables S1 and 2 contain crystallographic data and select geometric parameters. The Hg(II) center is seven-coordinate, including one weakly bound perchlorate ion which has a Hg–O(1) distance of 2.715 (5) Å. The stereochemistry of the Hg(II) center is that of a C_{2v} capped trigonal prism. The tertiary amine Hg–N(1) and –N(2) bond lengths are 2.470(5) Å and 2.434(5) Å and the bonds between the Hg(II) center and the pyridyl groups are shorter, ca. 2.35 Å, and similar in length to that in [Hg(beppa)ClO_4)]ClO_4.[66]

Figure 7 depicts the results of metal ion selectivity studies for MS5 at pH 7. The selectivity is analogous to that observed for MS1,[34] with only Cu(II) interfering with the fluorescence response to Hg(II). Variations in pH from 7 – 9 have no effect of the observed selectivity, which is also independent of ionic strength and the choice of anion in the buffer.

Simultaneous Detection of Hg(II) and Zn(II)

Multi-analyte sensing is important for simultaneously determining the presence of various components in a mixture.[67] We therefore determined whether MS5 could perform in combination with an Hg(II)-insensitive fluoroionophore to detect multiple metal ions in aqueous solution. We choose a fluorescein-based Zn(II) sensor, QZ2 (Figure 1), which has a Hg(II)-insensitive emission and affords fluorescence enhancement for Zn(II) in the presence of Hg(II).[68] Figure 8 depicts the response of a MS5/QZ2 mixture in the presence of Hg(II), Zn(II) and both Hg(II) and Zn(II) at pH *7*. Independent fluorescence changes of MS5 and QZ2 are observed in the presence of only Hg(II) or Zn(II), respectively. When a mixture of Hg(II) and Zn(II) is added, both sensors respond independently to their respective analytes. The rise centered at 624 nm indicates the presence of Hg(II) and that centered at 520 nm signals Zn(II). This experiment demonstrates that MS5 can be employed in conjunction with a sensor emitting at shorter wavelengths for multi-analyte detection.

MS5 Performance in Natural Water Samples

Small molecule fluorescence detectors for Hg(II) have the potential for use in the field. Such an application presents a unique set of challenges and requires detailed studies of sensor performance in the environmental milieu and method/device design. As a first step towards the former objective, we tested the ability of MS5 to respond to Hg(II) in natural water. Samples were collected from three sources, including the Charles River (Cambridge, MA), and representative data are given in Figure 9. In each case, MS5 shows ~4.5-fold or greater fluorescence turn-on in samples spiked with Hg(II). This result indicates that MS5 can detect Hg(II) in solutions with significantly more complex composition than laboratory buffer and suggests that its sensitivity to chloride ion will not be a limiting factor for use in environmental monitoring.

Summary

This work describes the synthesis and characterization of mercury sensor MS5. This sensor was designed to afford low-energy emission, both turn-on and ratiometric fluorescence responses to Hg(II), and a high degree of Hg(II) ion selectivity. The solution studies show that pH is a key factor for generating a ratiometric response to Hg(II). We propose that this behavior reflects the requirement of the seminaphthofluorescein dianion for significant enhancement of the 624 nm band, although more detailed physical characterization is needed to address this notion. It became evident during our investigation that the fundamental chemistry of seminaphthofluorescein is relatively unexplored.[69] Detailed investigations of its protonation and tautomeric equilibria and fluorescence behavior in a number of different solvent systems will be especially helpful in both creating new red-emitting chromophores with enhanced

brightness at neutral pH and guiding future sensor design. MS5 gives selective fluorescent enhancement for Hg(II), binds Hg(II) rapidly and reversibility, and has a lower detection limit of 50 nM at pH 7. Preliminary studies in natural water samples indicate that MS5 offers immediate Hg(II) detection in complex media. This observation points to its potential utility in the field.

Supplementary Material

Refer to Web version on PubMed Central for supplementary material.

Acknowledgements

This work was supported by Grant GM65519 from the National Institute of General Medical Sciences. E.M.N. thanks the Whitaker Health Science Fund for a graduate fellowship, Ms. C. W. Nolan for collecting water samples, Drs. D. Song and R. P. Feazell for assistance with the crystal structure determinations and Professor C. Fahrni for a helpful discussion.

References

1. Renzoni A, Zino F, Franchi E. Environ Res Sec A 1998;77:68–72.
2. Nendza M, Herbst T, Kussatz C, Gies A. Chemosphere 1997;35:1875–1885. [PubMed: 9353909]
3. Bolger PM, Schwetz BA. New Eng J Med 2002;347:1735–1736. [PubMed: 12456847]
4. Harris HH, Pickering IJ, George GN. Science 2003;301:1203. [PubMed: 12947190]
5. Boening DW. Chemosphere 2000;40:1335–1351. [PubMed: 10789973]
6. Clarkson TW, Magos L, Myers GJ. New Eng J Med 2003;349:1731–1737. [PubMed: 14585942]
7. Fan LJ, Zhang Y, Jones WE. Marcomolecules 2005;38:2844–2849.
8. Kim IB, Bunz UWFJ. Am Chem Soc 2006;128:2818–2819.
9. Zhao Y, Zhong ZJ. Am Chem Soc 2006;128:9988–9989.
10. Cheng P, He CJ. Am Chem Soc 2004;126:728–729.
11. Ono A, Togashi H. Angew Chem Int Ed 2004;43:4300–4302.
12. Matsushita M, Meijler MM, Wirsching P, Lerner RA, Janda KD. Org Lett 2005;7:4943–4946. [PubMed: 16235928]
13. Chae MY, Czarnik AWJ. Am Chem Soc 1992;114:9704–9705.
14. Yoon J, Ohler NE, Vance DH, Aumiller WD, Czarnik AW. Tetrahedron Lett 1997;38:3845–3848.
15. Hennrich G, Sonnenschein H, Resch-Genger UJ. Am Chem Soc 1999;121:5073–5074.
16. Prodi L, Bargossi C, Montalti M, Zaccheroni N, Su N, Bradshaw JS, Izatt RM, Savage PBJ. Am Chem Soc 2000;122:6769–6770.
17. Rurack K, Kollmannsberger M, Resch-Genger U, Daub JJ. Am Chem Soc 2000;122:968–969.
18. Hennrich G, Walther W, Resch-Genger U, Sonnenschein H. Inorg Chem 2001;40:641–644. [PubMed: 11225105]
19. Sakamoto H, Ishikawa J, Nakao S, Wada H. Chem Commun 2001:2395–2396.
20. Guo X, Qian X, Jia LJ. Am Chem Soc 2004;126:2272–2273.
21. Métivier R, Leray I, Valeur B. Chem Eur J 2004;10:4480–4490.
22. Dickerson TJ, Reed NN, LaClair JJ, Janda KDJ. Am Chem Soc 2004;126:16582–16586.
23. Zhang G, Zhang D, Yin S, Yang X, Shuai Z, Zhu D. Chem Commun 2005:2161–2163.
24. Liu B, Tian H. Chem Commun 2005:3156–2158.
25. Caballero A, Martínez R, Lioveras V, Ratera I, Vidal-Gancedo J, Wurst K, Tárraga A, Molina P, Veciana JJ. Am Chem Soc 2005;127:15666–15667.
26. Ros-Lis JV, Marcos MD, Mártinez-Máñez R, Rurack K, Soto J. Angew Chem Int Ed 2005;44:4405–4407.
27. Chen QY, Chen CF. Tetrahedron Lett 2005;46:165–168.
28. Moon SY, Youn NJ, Park SM, Chang SKJ. Org Chem 2005;70:2394–2397.

29. Yu Y, Lin LR, Yang KB, Zhong X, Huang RB, Zheng LS. Talanta 2006;69:103–106.
30. Kim SH, Kim JS, Park SM, Chang SK. Org Lett 2006;8:371–374. [PubMed: 16435837]
31. Kim SH, Song KC, Ahn S, Kang YS, Chang SK. Tetrahedron Lett 2006;47:497–500.
32. Song KC, Kim JS, Park SM, Chung K-C, Ahn S, Chang SK. Org Lett 2006;8:3413–3416. [PubMed: 16869623]
33. Czarnik AW. Ace Chem Res 1994;27:302–308.
34. Nolan EM, Lippard SJJ. Am Chem Soc 2003;125:14270–14271.
35. Nolan EM, Lippard SJJ. Mater Chem 2005;27–28:2778–2783.
36. Mello JV, Finney NSJ. Am Chem Soc 2005;127:10124–10125.
37. Yang YK, Yook KJ, Tae JJ. Am Chem Soc 2005;127:16760–16761.
38. Wang J, Qian X. Chem Commun 2006:109–111.
39. Yoon S, Albers AE, Wong AP, Chang CJJ. Am Chem Soc 2006;127:16030–16031.
40. Zheng H, Qian ZH, Xu L, Yuan FF, Lan LD, Xu JG. Org Lett 2006;8:859–861. [PubMed: 16494459]
41. Wang J, Qian X, Cui JJ. Org Chem 2006;71:4308–4311.
42. Wang J, Xuhong Q. Org Lett 2006;8:3721–3724. [PubMed: 16898801]
43. Nolan EM, Racine ME, Lippard SJ. Inorg Chem 2006;45:2742–2749. [PubMed: 16529499]
44. Ko SK, Yang WK, Tae J, Shin IJ. Am Chem Soc 2006;128:14150–14155.
45. Descalzo AB, Martinez-Manez R, Radeglia R, Rurack K, Soto JJ. Am Chem Soc 2003;125:3418–3419.
46. Rurack K, Resch-Genger U, Bricks JL, Spieles M. Chem Commun 2000:2103–2104.
47. Zhu XJ, Fu ST, Wong WK, Guo JP, Yong WY. Angew Chem Int Ed 2006;45:3150–3154.
48. Chang CJ, Jaworski J, Nolan EM, Sheng M, Lippard SJ. Proc Natl Acad Sci USA 2004;101:1129–1134. [PubMed: 14734801]
49. SMART: Software for the CCD Detector System, version 5.626. Bruker AXS; Madison, WI: 2000.
50. Kuzelka J, Mukhopadhyay S, Spingler B, Lippard SJ. Inorg Chem 2004;43:1751–1761. [PubMed: 14989668]
51. Sheldrick, GM. SADABS: Area-Detector Absorption Correction. University of Gottingen; Gottingen, Germany: 2001.
52. SAINTPLUS: Software for the CCD Detector System, version 5.01. Bruker AXS; Madison, WI: 1998.
53. SHELXTL: Program Library for Structure Solution and Molecular Graphics, version 6.1. Bruker AXS; Madison, WI: 2001.
54. Spek, A. PLATON, A Multipurpose Crystallographic Tool. Utrecht University; Utrecht, The Netherlands: 2000.
55. Brannon JH, Madge DJ. Phys Chem 1978;82:705–709.
56. Whitaker JE, Haugland RP, Prendergast FG. Anal Biochem 1991;194:330–344. [PubMed: 1862936]
57. Sjöback R, Nygren J, Kubista M. Spectrochimica Acta Part A 1995;51:L7–L21.
58. Nolan EM, Lippard SJ. Unpublished results
59. de Silva AP, Gunaratne HQN, Gunnlaugsson T, Huxley AJM, McCoy CP, Rademacher JT, Rice TE. Chem Rev 1997;97:1515–1566. [PubMed: 11851458]
60. Callan JF, de Silva AP, Magri DC. Tetrahedron 2005;61:8551–8588.
61. Wright JG, Natan FM, MacDonnell FM, Ralston DM, O'Halloran TV. Prog Inorg Chem 1990;38:323–412.
62. A 500 nM concentration of MS5 was employed because we were unable to obtain reliable data with lower concentrations and 4 nm slit widths.
63. Anderegg, vG; Hubmann, E.; Fodder, NG.; Wenk, F. Helv Chim Acta 1977;60:123–140.
64. Coronado E, Gálan-Mascarós JR, Martí-Gastaldo C, Palomares E, Durrant JR, Vilar R, Gratzel M, Nazeeruddin MKJ. Am Chem Soc 2005;127:12351–12356.
65. Mikata Y, Wakamatsu M, Yano S. Dalton Trans 2005:545–550. [PubMed: 15672199]
66. Makowska-Grzyska MM, Doyle K, Allred RA, Arif AM, Bebout DC, Berreau LM. Eur J Inorg Chem 2005:822–827.

67. Walt DR. Current Opin Chem Biol 2002;6:689–695.

68. Nolan EM, Jaworski J, Okamoto KI, Hayashi Y, Sheng M, Lippard SJJ. Am Chem Soc 2005;127:16812–16823.

69. A SciFinder search yielded only 39 hits and only 116 for “seminaphthofluorescein” and only 115 for “SNAFL” compared to over 60,000 hits generated by “fluorescein” in November of 2006.

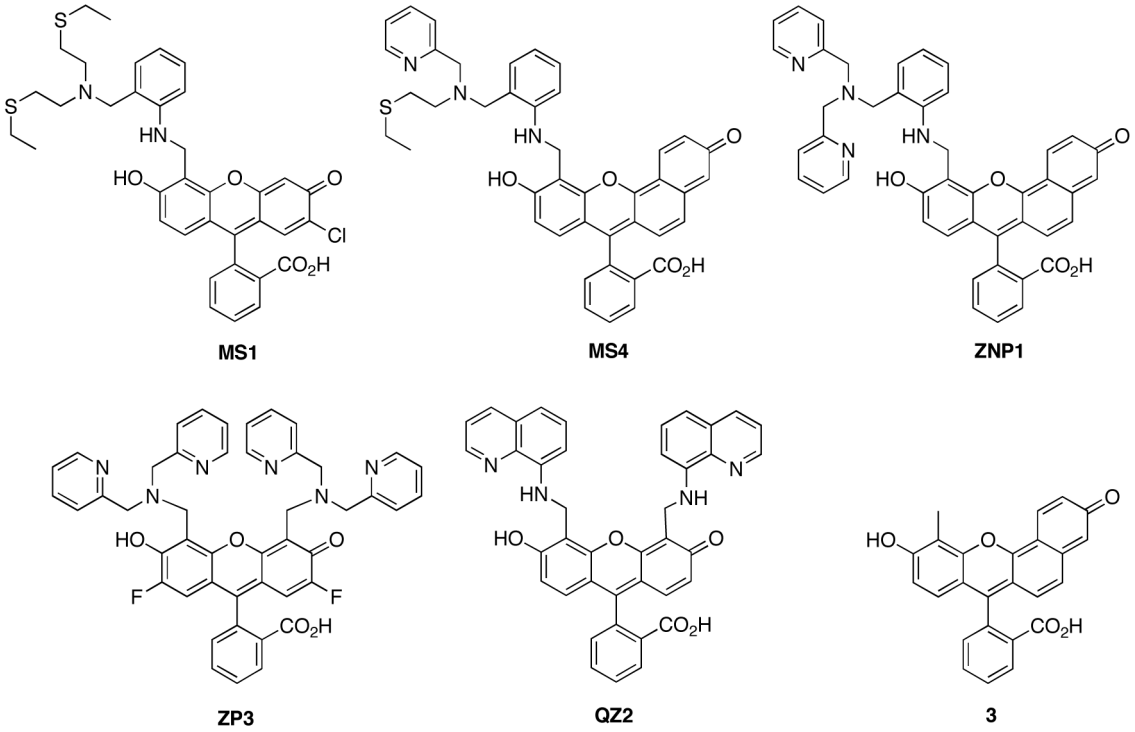

Figure 1.
Structures of metal ion sensors and seminaphthofluorescein **3**

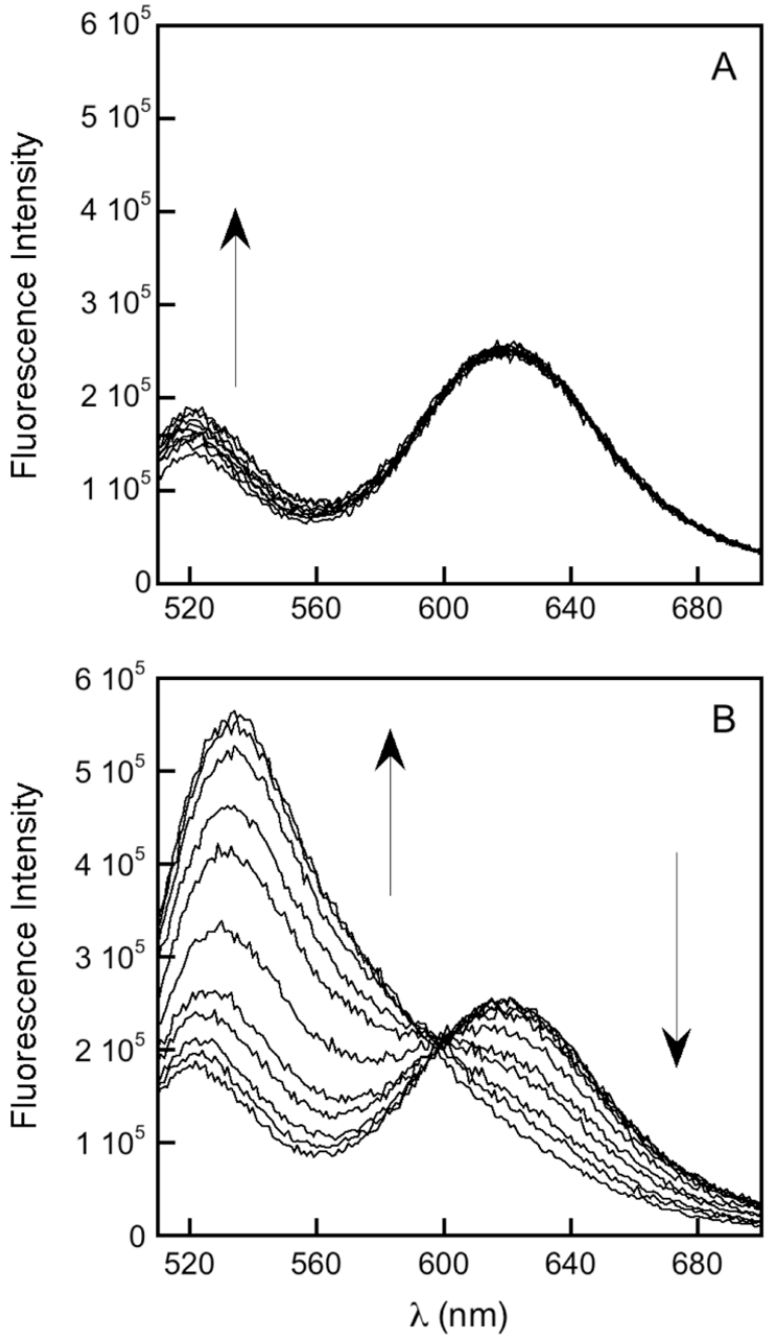

Figure 2.
Effect of pH on the emission ot 5 μM MS5 (100 mM KCl, λ_{ex} = 499 nm, T = 25 °C). A. The pH was decreased from ~12 to ~9 in increments of ~0.25. B. The pH was decreased from ~9 to ~6 in increments of ~0.25. See Figure S4 for data taken at pH < 6.

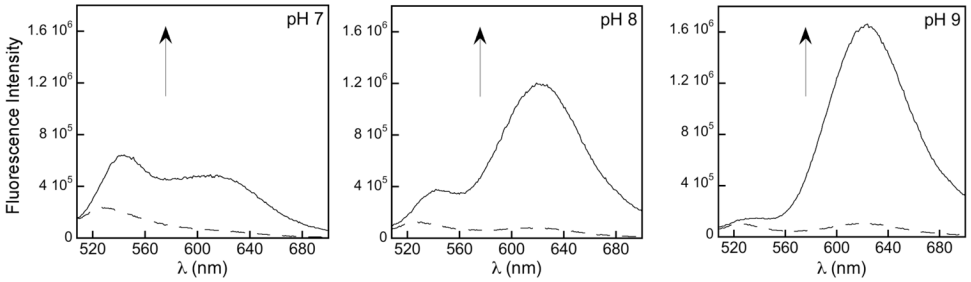

Figure 3.

Fluorescence response of MS5 to Hg(II) as a function of pH. The dotted lines represent the emission from 5 μM MS5 at pH 7 (50 mM PIPES, 100 mM KCl), pH 8 (50 mM HEPES, 100 mM KCl) and 9 (50 mM CHES, 100 mM KCl). The solid lines represent the emission change that occurs immediately upon addition of 20 equiv of $HgCl_2$. The samples were excited at 499 nm and T = 25 °C.

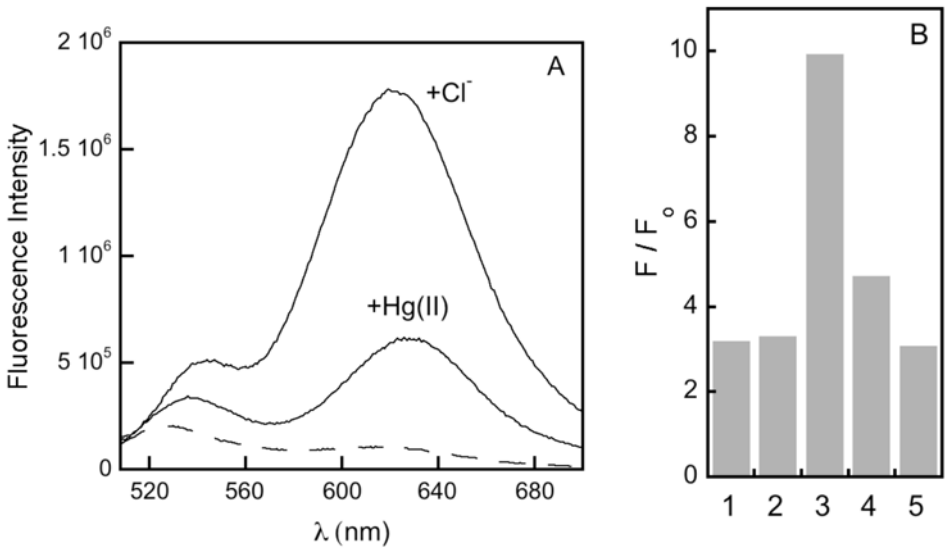

Figure 4.

Effect of anions on the emission of the MS5:Hg(II) complex. A. The dashed line represents the emission from 5 μM MS5 in the absence of chloride ion (50 mM HEPES, pH 8). Addition of 20 equiv of Hg(II) results in ~3-fold fluorescence enhancement. Full emission is restored immediately after addition of aqueous KCl (final concentration = 100 mM). B. The effect of various anions in the buffer (50 mM HEPES, 100 mM KX, pH 8): **1**, no potassium salt; **2**, KNO_3; **3**, KCl; **4**, KOAc; **5**, KF. F is the fluorescence observed after Hg(II) addition and F_o is the emission from free MS5. The samples were excited at 499 nm and T = 25 °C.

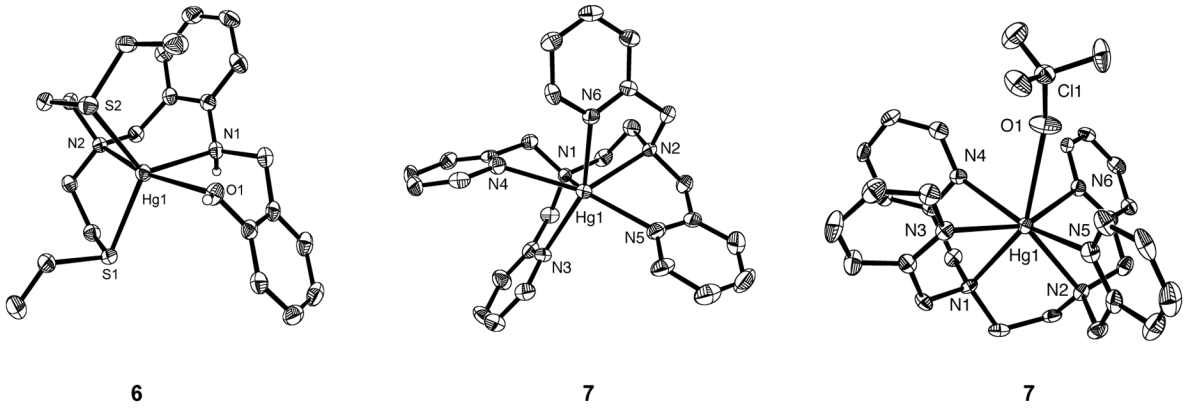

6 **7** **7**

Figure 5.

ORTEP diagrams of the Hg(II) complexes **6** and **7**. The ORTEP diagrams of **6** and **7** depict the 40% probability thermal ellipsoids for all non-hydrogen atoms. The left and middle ORTEP diagrams omit the perchlorate counterions. The right-most ORTEP diagram of **7** illustrates the orientation of the weakly associated perchlorate anion. The Hg(1)–O(1) distance is 2.715(5) Å.

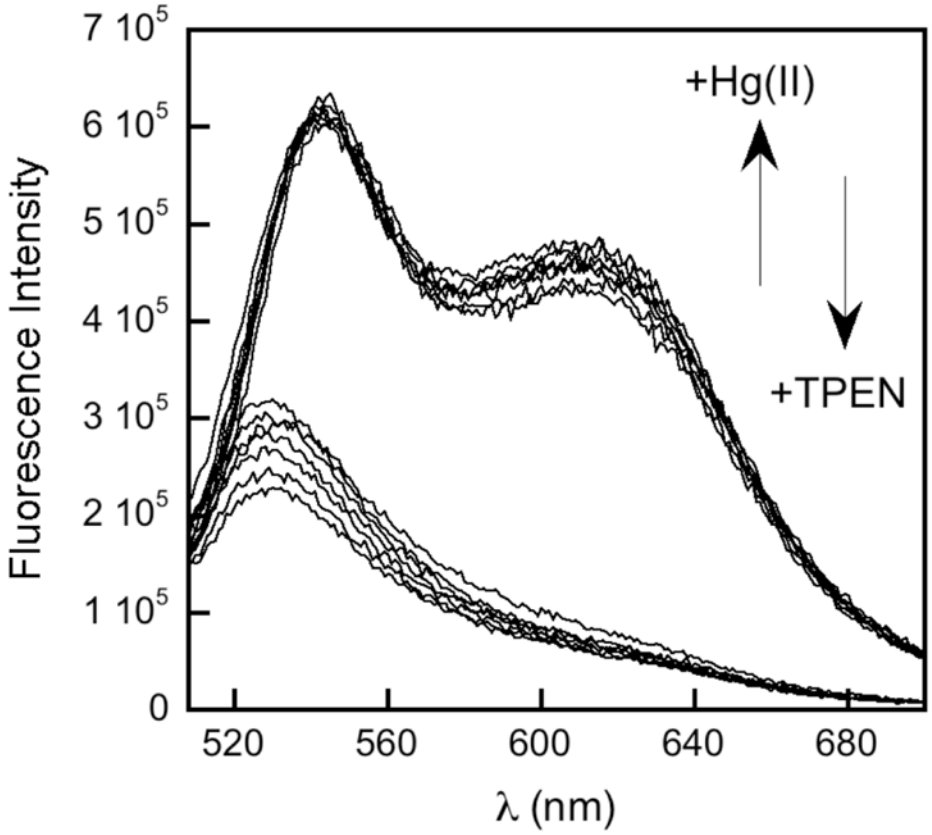

Figure 6.

Reversibility of Hg(II) coordination to 5 μM MS5 by TPEN addition (50 mM PIPES, 100 mM KCl, pH 7). The top set of solid lines represent the fluorescence enhancement that occurs immediately after addition of 10 equiv of Hg(II). The bottom set of solid lines represents the emission from free MS5 and the emission decreases that occur immediately after addition of 10 equiv of TPEN to a solution containing the MS5:Hg(II) complex. Six cycles of on/off by Hg(II)/TPEN addition are depicted in this plot and the slight fluorescence rise observed in the bottom spectra ca. 530 nm results from TPEN emission (control data not shown). The samples were excited at 499 nm and T = 25 °C.

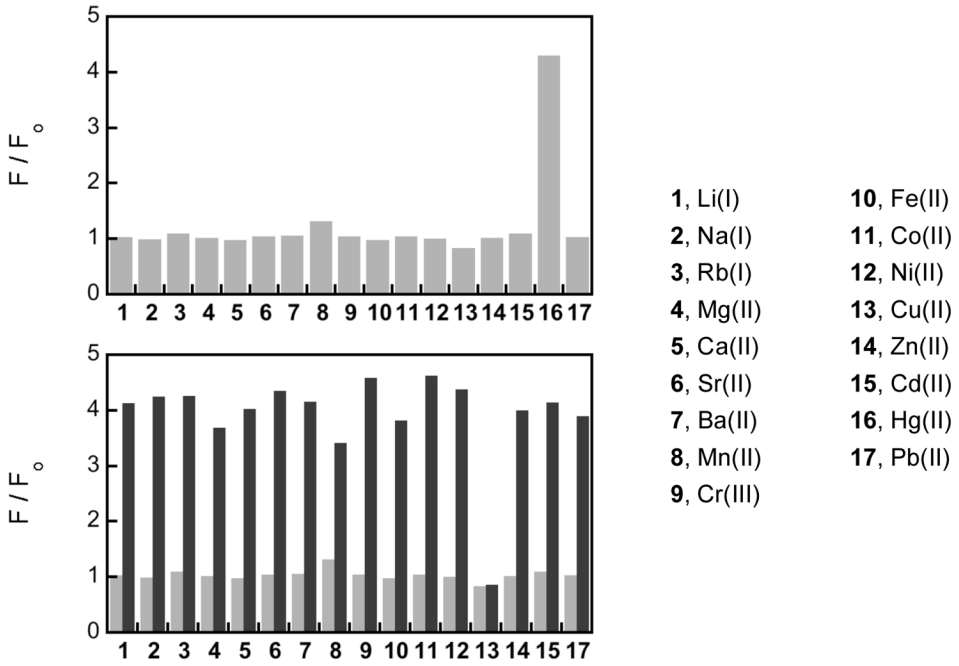

Figure 7.

Selectivity of MS5 for Hg(II) over other cations at pH 7 (50 mM PIPES, 100 mM KCl). Top plot: Fluorescence response of 5 μM MS5 following addition of 20 equiv of the cation of interest: 1, LiCl; 2, NaCl; 3, RbCl; 4, $MgCl_2$; 5, $CaCl_2$; 6, $SrCl_2$; 7, $BaCl_2$; 8, $MnCl_2$; 9, $Cr(CH_3CO_2)_3$; 10, $Fe(NH_4)_2(SO_4)_2$; 11, $CoCl_2$; 12, $NiCl_2$; 13, $Cu(SO_4)_2$; 14, $ZnCl_2$; 15, $CdCl_2$; 16, $HgCl_2$; 17, $Pb(NO_3)_2$. Bottom plot: The light grey bars correspond to the bars in the top plot. The black bars indicate the fluorescence change that occurs immediately following addition of 20 equiv of Hg(II) to the solutions containing MS5 and the cation of interest. All data (F) were normalized with respsect to emission of the free sensor (F_0). The samples were excited at 499 nm and the emission integrated from 505 – 700 nm. T = 25 °C. MS5 is also selective for Hg(II) in the presence of millimolar concentrations of the alkali and alkaline earth metals (data not shown).

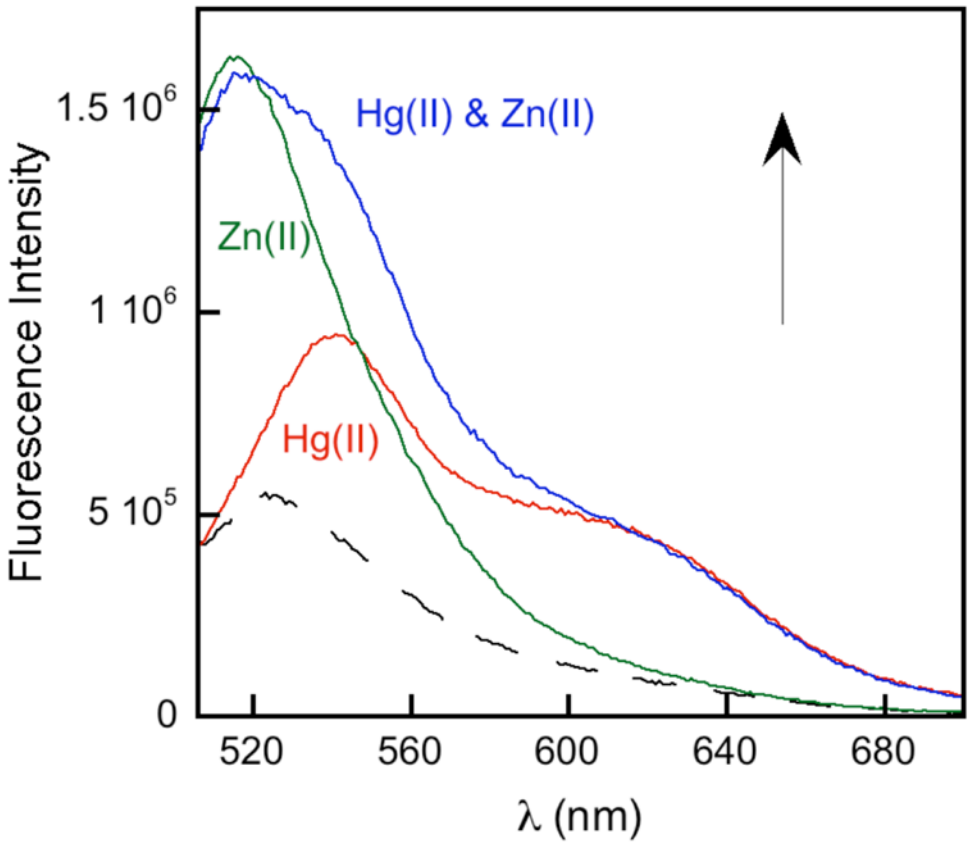

Figure 8.

Fluorescence response to Hg(II) and Zn(II) from a mixture of 5 μM MS5 and 100 nM QZ2 at pH 7 (50 mM PIPES, 100 mM KCl). The black dashed line represents emission from the MS5/QZ2 mixture. The red line is the emission from the mixture immediately after addition of only 50 μM Hg(II). The green line is the emission from the mixture immediately after addition of only 50 μM Zn(II). The blue line is the response in the presence of both 50 μM Hg(II) and Zn (II). The samples were excited at 499 nm and T = 25 °C.

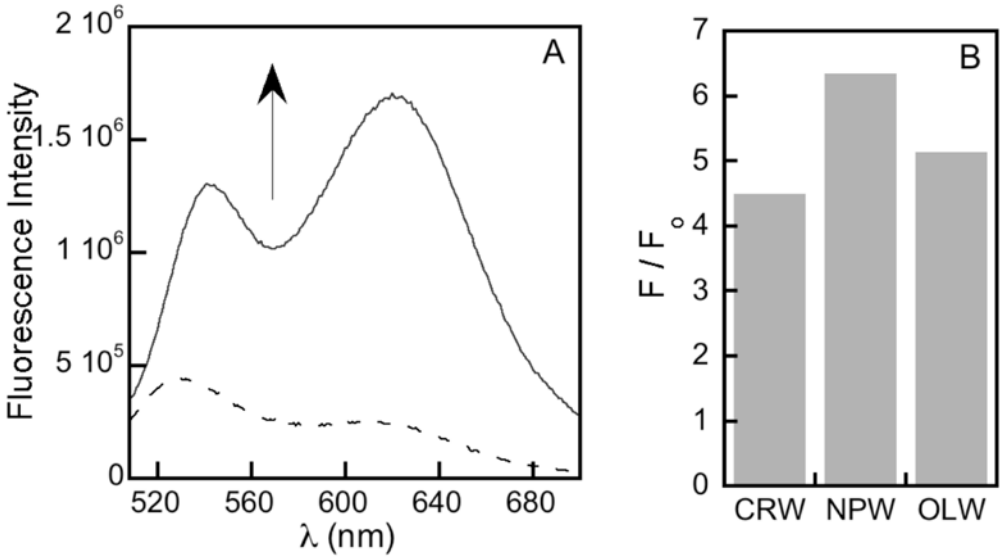

Figure 9.

Response of 5 μM MS5 to 10 equiv of Hg(II) added to natural water samples. A. Emission spectra for MS5 in Charles River water before (dashed line) and after (solid line) addition of 10 equiv of Hg(II). B. Fluorescence response of MS5 to Hg(II) in Charles River water (CRW), Newburyport water (NPW) and Onondaga Lake water (OLW). The response (F) is normalized to the emission of the free sensor (F_0). The samples were excited at 499 nm and T = 25 °C.

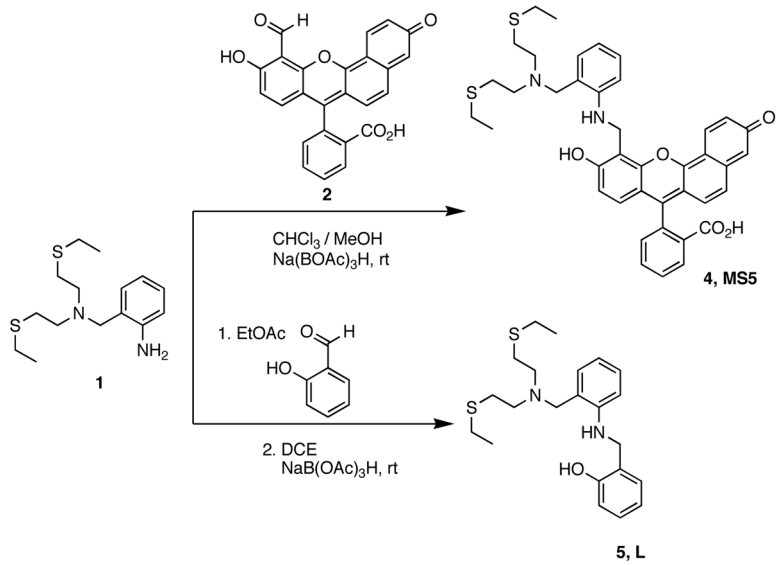

Scheme 1.
Synthesis of MS5 and its salicylaldehyde-based analog **L**.

Table 1

Spectroscopic Properties of MS5[a]

PH	Absorption λ(nm); ε × 10^3 ($M^{-1}cm^{-1}$)		Emission λ (nm); Φ[b]	
	Unbound	Hg(II)	Unbound	Hg(II)
7	500 4.5; 528, 4.5	492, 7.0; 533, 7.8	536, 611; 0.018	524, 612; 0.032
8	531, 12.2	541, 16.0	532, 612; 0.009	546, 624; 0.064
9	552, 24.2	547, 27.2	522, 620; 0.010	534, 624; 0.086

[a] All measurements were made in the presence of 100 mM KCl and with 50 mM PIPES (pH 7), 50 mM HEPES (pH 8), 50 mM CHES (pH 9), or 50 mM CAPS (pH 11) buffer.

[b] Fluorescein (**Φ** = 0.95 in 0.1 N NaOH, ref. [55]) was used as the standard for the quantum yield measurements.

Table 2

Selected Interatomic Distances (A) and Angles (deg)[a]

			$[Hg(L)_2](ClO_4)_2 \cdot CH_3OH$ (6)		
Hg1-N1	2.334(3)	N1-Hg1-O1	79.18(9)	N2-Hg1-S1	83.18(6)
Hg1-N2	2.436(3)	N1-Hg1-S1	114.59(7)	N2-Hg1-S2	83.35(6)
Hg1-S1	2.5076(8)	N1-Hg1-S2	120.97(7)	O1-Hg1-S1	105.42(6)
Hg1-S2	2.4854(8)	N1-Hg1-N2	87.97(9)	O1-Hg1-S2	100.05(6)
Hg1-O1	2.572(3)	N2-Hg1-O1	166.63(8)	S1-Hg1-S2	121.98(3)
		[Hg(TPEN)]$(ClO_4)_2$ (7)			
Hg1-N1	2.470(5)	N1-Hg1-N3	72.97(18)	N2-Hg1-N6	72.45(17)
Hg1-N2	2.434(5)	N1-Hg1-N4	70.86(16)	N3-Hg1-N4	73.57(17)
Hg1-N3	2.337(5)	N1-Hg1-N5	123.49(17)	N3-Hg1-N5	99.54(18)
Hg1-N4	2.572(5)	N1-Hg1-N6	109.31(18)	N3-Hg1-N6	153.11(18)
Hg1-N5	2.360(5)	N2-Hg1-N3	131.58(17)	N4-Hg1-N5	162.29(18)
Hg1-N6	2.357(5)	N2-Hg1-N4	126.37(17)	N4-Hg1-N6	81.85(17)
N1-Hg1-N2	74.55(17)	N2-Hg1-N5	70.53(18)	N5-Hg1-N6	100.74(18)

[a] Atoms are labeled as indicated in Figures 5, S5 and S7.

J Am Chem Soc. Author manuscript; available in PMC 2008 August 11.